EVALUATION OF YIELD ACCELERATION FACTOR
OF EARTH-SLOPES BY LIMIT ANALYSIS

BY

Tomoyuki SAWADA*, Sumio G. NOMACHI**
and Wai F. CHEN***
(Received 30 November 1982)

SYNOPSIS

The upper bound technique of limit analysis of perfect plasticity is applied to evaluate the stability of slopes induced by earthquake load. The analysis considers the following cases.

1) homogeneous and isotropic slope
2) effect of upper slope angle α

The computer models developed are based on the following conditions.

1) plane strain
2) plane and log-spiral failure surfaces
3) pseudo-static earthquake loading
4) uniform horizontal distribution of lateral acceleration
5) Coulomb creterion for failure with constant c and ϕ.

I. Introduction

The conventional method for evaluating the effect of an earthquake load on the stability of a slope is the so-called "pseudo-static method of analysis". In this analysis, the inertia force is treated as an equivalent concentrated horizontal force (the "pseudo-static force") at some critical point (usually the center of gravity) of the critical sliding mass. The inadequacies of this method for slope stability analysis are discussed in various papers by many authors (for example, see Chen , 1982). Despite these criticisms, the pseudo-static method continues to be used by consulting geotechnical engineers because it is required by the building codes, it is easier and less costly to apply, and satisfactory results have been obtained since 1933. This method will continue to be popular until an alternative method can be shown to be a more reasonble approach.

In this study, the upper bound technique of limit analysis (Chen, 1975) is applied. The limit analysis method is based on the assumption that soil deformations follow the flow rule associated with the Coulomb yield condition. This idealization requires that a plastic shearing deformation must be accompanied by an increase in volume. Thus, the rigid body type of sliding of a soil mass must occur

* Dept. of Civil Engneering Assoc. Prof.
** Hokkaido UNIVERSITY
Dept. of Civil Engineering Professor
*** Purdue UNIVERSITY
Dept. of Civil Engineering Professor & Head of Structural Engr.

discontinuously with an angle ϕ between the velocity vector and the discontinuous slip surface (Chen, 1975).

At the state of collapse, the rate of work done by the external loads must exceed or at least equal to the internal rate of energy dissipation along the critical slip surface including its own weight as well as the inertia force induced by earthquake force. By equating the external rate of work to the internal rate of energy dissipation for an assumed failure mechanism, we obtain an upper bound solution to the yield acceleration coefficient factor, K_c.

The effect of an earthquake load on a potential sliding mass is now expressed in terms of an equivalent static horizontal force determined as the product of a seismic coefficient factor K, and the weight of the potential sliding mass.

Herein, we are concerned with the calculation of the critical or yield horizontal force correspond-inertiaing to the yield acceleration factor K_c, at which a condition of incipient slope movement is possible along the potential sliding surface.

In this paper, the computation of the yield acceleration factor K_c by the upper bound technique of limit analysis is based on the following three possible local failure mechanisms,

(1) Plane failure mechanism

(2) Log-spiral failure mechanism passing through the toe

(3) Log-spiral failure mechanism passing below the toe

II. Plane Failure Mechanism for a Homogeneous and Isotropic slope

Figure 1 shows the first of the three possible failure Mechanisms i. e. plane failure mechanism. Region ABC translates as a rigid body with the velocity v which makes an angle ϕ to the slip surface AC. The failure mechanism is assumed to end at point C in Fig. 1 with the vertical height $H+L\sin\alpha$.

The failure mechanism is defined by the angle of slip surface θ. The length L is related to the

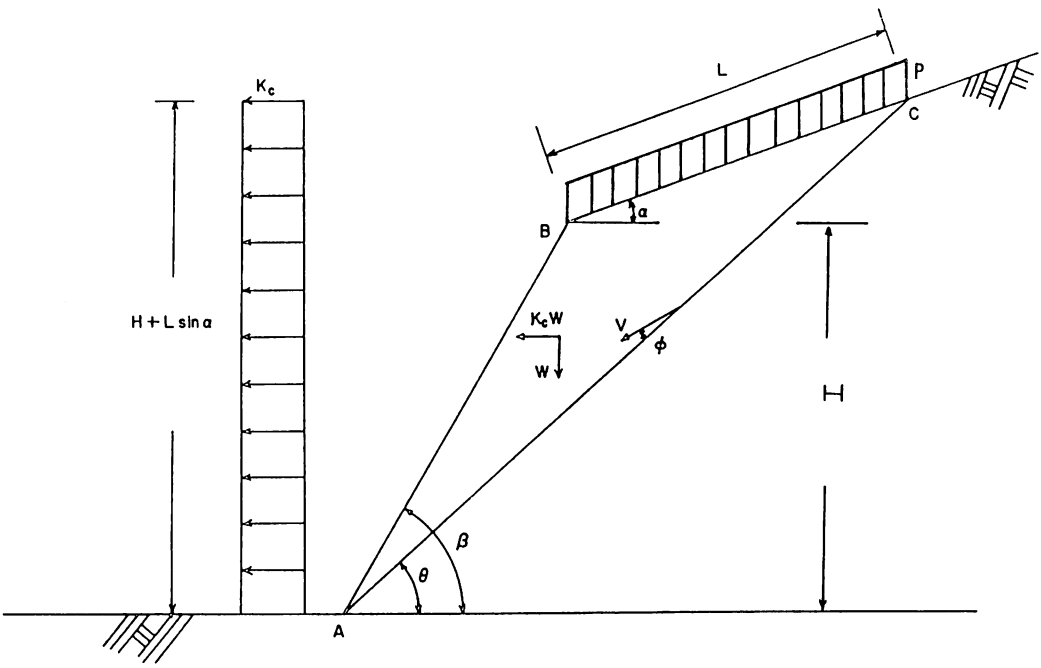

Fig. 1 Translational Local Slope Failure Mechanism with an upper slope angle : α

slope angles α, β and slope height H as

$$L=\frac{H\sin(\beta-\theta)}{\sin\beta\sin(\theta-\alpha)} \tag{1}$$

The rate of internal energy dissipation along the slip surface AC is found by multiplying the length of the slip surface by C times the discontinuity in velocity, V$\cos\phi$ (Chen, 1975) where c is cohesion and ϕ is internal friction angle of soil as defined in the Coulomb yield condition.

$$c\left(\frac{H+L\sin\alpha}{\sin\theta}\right)V\cos\phi \tag{2}$$

The rate of external work done by the soil weight of the sliding mass with unit weight, γ is

$$\frac{1}{2}HL\left(\cos\alpha-\frac{\sin\alpha}{\tan\beta}\right)\gamma V\sin(\theta-\varphi) \tag{3}$$

by the surcharge load with intensity P is,

$$(PL)\ V\sin(\theta-\phi) \tag{4}$$

and by the inertia force with seismic coefficients xK_c is

$$K_c\frac{1}{2}HL\left(\cos\alpha-\frac{\sin\alpha}{\tan\beta}\right)\gamma V\cos(\theta-\phi) \tag{5}$$

$$xK_c(pL)\ V\cos(\theta-\phi) \tag{6}$$

where xK is the yield acceleration factor corresponding to the surcharge load p whose magnitude can be related to the yield acceleration factor of the sliding soil weight, K, through the coefficient, x. The value of x can be near unit.

By equating the total external rates of work to the internal rate of dissipation, an upper bound value of K is obtained

$$K=F(\theta) \tag{7}$$

$$=\frac{\dfrac{c\cos\phi\sin(\beta-\alpha)}{\sin(\beta-\theta)\cos(\theta-\phi)}-p\tan(\theta-\phi)-\dfrac{\gamma H}{2}\dfrac{\sin(\beta-\alpha)}{\sin\beta}\tan(\theta-\phi)}{\dfrac{\gamma H}{2}\dfrac{\sin(\beta-\alpha)}{\sin\beta}+px}$$

The function F(θ) has a minimum value when θ satisfies the condition

$$\frac{\partial F}{\partial\theta}=0 \tag{8}$$

Solving Eq. (8) and substituting θ so obtained into Eq. (7), we obtain the least upper bound solution for the yield acceleration factor, K_c corresponding to the failure mechanism shown in Fig. 1.

$$K_c=\min.\ F(\theta) \tag{9}$$

III. Log-spiral Failure Mechanism for a Homogeneous and Isotropic slope

The plane failure mechanism of Fig. 1 is a translation type of sliding. Herein, we consider two cases of rotational log-spiral failure mechanism : One passing through the toe (Fig. 2) and the other

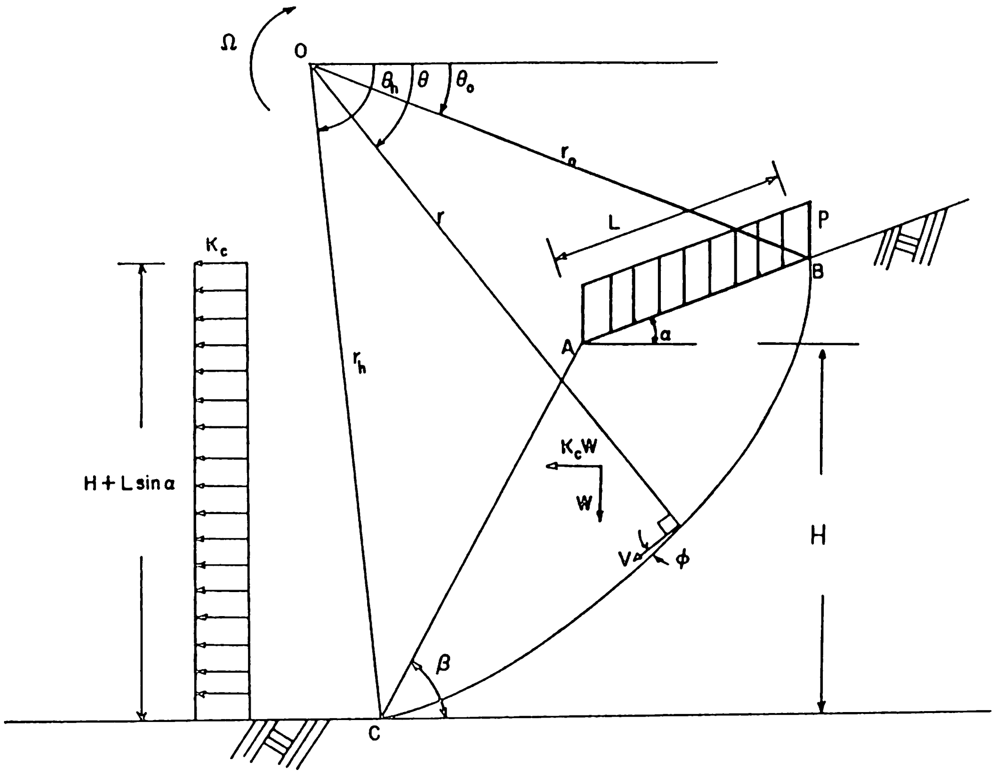

Fig. 2 Rotational Local Slope Failure Mechanism with an upper slope angle : α (passing through the too)

below the toe (Fig. 3). The region ABC or ABC′C rotates as a rigid body about the as yet undefined center of rotation O with the angular velocity Ω relative to the materials below the logarithmic failure surface BC or BC′. Here, as inprevious work (Chen et al, 1969, 1971) the parameters H, θ_o and θ_h are used to define the failure mechanism.

Case 1 : slip surface passing through the toe

Figure 2 shows the case of sliding through the toe.

The geometrical relation between L and H is

$$\frac{H}{r_o}=\frac{\sin\beta}{\sin(\beta-\alpha)}\{\sin(\theta_h+\alpha)\exp[(\theta_h-\theta_o)\tan\phi]-\sin(\theta_o+\alpha)\tag{10}$$

$$\frac{L}{r_o}=\frac{\sin(\theta_h-\theta_o)}{\sin(\theta_h+\alpha)}-\frac{\sin(\theta_h+\beta)}{\sin(\theta_h+\alpha)\sin(\beta-\alpha)}$$

$$\{\sin(\theta_h+\alpha)\exp[(\theta_h+\theta_o)\tan\phi]-\sin(\theta_o+\alpha)\}\tag{11}$$

from which, we have

$$\frac{L}{H}=\frac{\sin(\theta_h-\theta_o)\sin(\beta-\alpha)}{\sin\beta\sin(\theta_h+\alpha)\{\sin(\theta_h+\alpha)\exp[(\theta_h-\theta_o)\tan\phi]-\sin(\theta_o+\alpha)\}}$$

$$-\frac{\sin(\theta_h+\beta)}{\sin\beta\sin(\theta_h+\alpha)}\tag{12}$$

The rate of internal sliding dissipation of energy occurred along the discontinuous sliding surface BC has the volum (Chen, 1975)

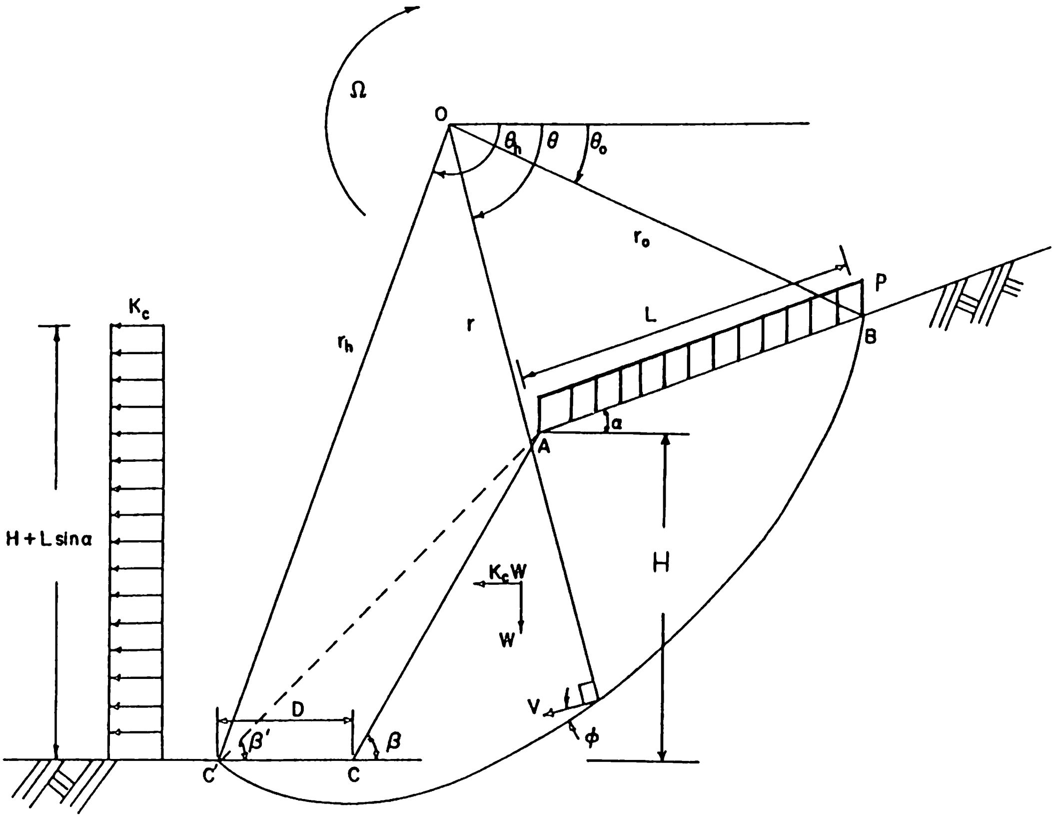

Fig. 3 Rotational Local Slope Failure Machanism with an upper slope : α (passing below the toe)

$$\int_s (c V_s) ds = \int_{\theta_o}^{\theta_h} (c V \cos\phi) \frac{r d\theta}{\cos\phi}$$

$$= \frac{c r_o^2 \Omega}{2\tan\phi} \{\exp[2(\theta_h - \theta_o)\tan\phi] - 1\}$$

$$= c r_o^2 \Omega F_c \tag{13}$$

The rate of external work due to soil weight for the region ABC can be found by a simple algebraic summation $\dot{Y}_1 - \dot{Y}_2 - \dot{Y}_3$, where $\dot{Y}_1$, $\dot{Y}_2$ and $\dot{Y}_3$ are the rates of work done by the soil weight in region OBC, OAB and OAC, respectively.

$$\dot{Y}_1 = \frac{\gamma r_o^3 \Omega}{3(1+9\tan^2\phi)} \{\exp[3(\theta_h - \theta_o)\tan\phi](3\tan\phi\cos\theta_h + \sin\theta_h) - 3\tan\phi \cos\theta_o - \sin\theta_o\}$$

$$= \gamma r_o^3 \Omega F_1 \tag{14}$$

$$\dot{Y}_2 = \frac{\gamma r_o^3 \Omega}{6} \frac{L}{r_o} (2 \cos\theta_o - \frac{L}{r_o} \cos\alpha) \sin(\theta_o + \alpha)$$

$$= \gamma r_o^3 \Omega F_2 \tag{15}$$

and

$$\dot{Y}_3 = \frac{r_o^3}{6} \exp[(\theta_h - \theta_o)\tan\phi]\{\sin(\theta_h - \theta_o) - \frac{L}{r_o} \sin(\theta_h + \alpha)$$

$$\times\{\cos\theta_o-\frac{L}{r_o}\cos\alpha+\cos\theta_h\exp[(\theta_h-\theta_o)\tan\phi])$$

$$=\gamma\ r_o^3\ \Omega\ F_3 \tag{16}$$

Similarly, the rate of work done by the inertia force on the soil weight can be found the simple summation by $\dot{Y}_4-\dot{Y}_5-\dot{Y}_6$, where $\dot{Y}_4$, $\dot{Y}_5$ and $\dot{Y}_6$ are the rates of work done by the horizontal inertia force due to soil weight in region OBC, OAB and OAC, respectively.

$$\dot{Y}_4=\frac{\gamma\ r_o^3\ \Omega\ K}{3(1+9\tan^2\phi)}\{(3\tan\phi\ \sin\theta_h-\cos\theta_h)\ \exp[3(\theta_h-\theta_o)\tan\phi]$$

$$-3\tan\phi\ \sin\theta_o+\cos\theta_o\}$$

$$=K\gamma\ r_o^3\ \Omega\ F_4 \tag{17}$$

$$\dot{Y}_5=\frac{\gamma\ r_o^3\Omega K}{6}\{2\ \frac{L}{r_o}\ \sin\theta_o+(\frac{L}{r_o})^2\ \sin\alpha\}\ \sin(\theta_o+\alpha)$$

$$=K\ \gamma\ r_o^3\ \Omega\ F_5 \tag{18}$$

and

$$\dot{Y}_6=\frac{\gamma\ r_o^3\Omega K}{6}\exp[(\theta_h-\theta_o)\tan\phi]\{\sin(\theta_h-\theta_o)-\frac{L}{r_o}\sin(\theta_h+\alpha)\}$$

$$\cdot\{\exp(\theta_h-\theta_o)\ \tan\phi\sin\theta_h+\sin\theta_o+\frac{L}{r_o}\ \sin\alpha\}$$

$$=K\ \gamma\ r_o^3\ \Omega\ F_6 \tag{19}$$

Further, the external rates of work due to the surcharge boundary load p and its associated inertia force are due to surcharge

$$p\ r_o^2\ \Omega\ \frac{L}{r_o}\ \cos\alpha(\cos\theta_o-\frac{L}{2r_o}\cos\alpha)$$

$$=p\ r_o^2\ \Omega\ F_p \tag{20}$$

due to inertia force of the surcharge

$$\mathrm{x}K\ pr_o^2\ \Omega\ \frac{L}{r_o}(\sin\theta_o+\frac{L}{2r_o}\sin\alpha)$$

$$=\mathrm{x}K\ pr_o^2\ \Omega\ F_q \tag{21}$$

By equating the rate of internal energy dissipation to the total rates of external work, we have

$$K=\frac{cF_c-\gamma r_o(F_1-F_2-F_3)-pF_p}{\gamma\ r_o(F_4-F_5-F_6)+\mathrm{x}PF_q} \tag{22}$$

that is

$$K=F(\theta_o,\theta_h)=\frac{cF_c-\dfrac{\sin(\beta-\alpha)}{\sin\beta}\dfrac{\gamma\ H(F_1-F_2-F_3)}{\{\sin(\theta_h+\alpha)\exp[(\theta_h-\theta_o)\ \tan\phi-\sin(\theta_o+\alpha\}]\}}-pF_p}{\dfrac{\sin(\beta-\alpha)}{\sin\beta}\dfrac{\gamma\ H(F_4-F_5-F_6)}{\{\sin(\theta_h+\alpha)\exp[(\theta_h-\theta_o)\tan\phi-\sin(\theta_o+\alpha)]\}}+\mathrm{x}pF_q} \tag{23}$$

The values of K as given in Eq. (23) are upper bound solutions for the yield acceleration factor corresponding to the log-spiral failure mechanism as shown in Fig. 2. Using the conditions

$$\frac{\partial F}{\partial \theta_o} = 0 \text{ and } \frac{\partial F}{\partial \theta_h} = 0 \tag{24}$$

and solving Eq. (24), we obtain the critical values of θ_o and θ_h which give the minimum value of K, or K_c as

$$K_c = \min.\ F(\theta_o, \theta_h) \tag{25}$$

Case 2 : slip surface passing below the toe

Figure 3 shows the case of failure surface passing below the toe. Similarly relations between D and H, and L and H can be found as

$$\frac{D}{H} = \frac{\sin(\beta-\beta')}{\sin\beta' \sin\beta} \tag{26}$$

$$\frac{H}{r_o} = \frac{\sin\beta'}{\sin(\alpha-\beta')} \{\sin(\theta_o+\alpha) - \exp[(\theta_h-\theta_o)\tan\phi)\tan\phi]\sin(\theta_h+\alpha)\} \tag{27}$$

$$\frac{L}{r_o} = \frac{\sin(\theta_h+\beta')}{\sin(\alpha-\beta')}\{\exp[(\theta_h-\theta_o)\tan\phi]-1\} \tag{28}$$

The rate of external work done by the region ABC′C can easily be obtained by first finding rates of work $\dot{Y}_1$, $\dot{Y}_2$, $\dot{Y}_3$ and $\dot{z}_1$ due to the soil weight in regions OBC′, OBA, OAC′ and ACC′, also $\dot{Y}_4$, $\dot{Y}_5$, $\dot{Y}_6$ and $\dot{z}_2$ due to the inertia force in each region respectively.

The functions $\dot{Y}_1$ to $\dot{Y}_6$ are the same as those given in expressions (14) to (19). The functions $\dot{z}_1$ and $\dot{z}_2$ resulting from the region ACC′ are given by (Fig. 3)

$$\dot{z}_1 = \gamma\ r_o^3\ \Omega\left(\frac{H}{r_o}\right) \frac{\sin(\beta-\beta')}{2\ \sin\beta\sin\beta'} \{\cos\theta_o - \frac{L}{r_o}\cos\alpha - \frac{1}{3}\left(\frac{H}{r_o}\right)(\cot\beta'+\cot\beta)\}$$

$$= \gamma\ r_o^3\ \Omega\ F_7 \tag{29}$$

and

$$\dot{z}_2 = K\gamma\, r_o^3 \left(\frac{H}{r_o}\right)^2 \frac{\sin(\beta-\beta')}{2\ \sin\beta\sin\beta'} \{\sin\theta_o + \frac{L}{r_o}\sin\alpha + \frac{2}{3}\left(\frac{H}{r_o}\right)\}$$

$$= K\ r_o^3\ \Omega\ F_8 \tag{30}$$

The external rates of work due to surcharge boundary load p and its associated inertia force must be added .These expressions are the same as those defined in Eq. (20) and (21). By equating the rate of internal energy dissipation to the total rates of external work through simple algebraic summation of $\dot{Y}$′s and $\dot{z}$′s, we obtain

$$K = \frac{cF_c - \gamma\ r_o(F_1 - F_2 - F_3 - F_7) - pF_p}{\gamma\ r_o(F_4 - F_5 - F_6 - F_8) + \mathrm{x}pF_q} \tag{31}$$

That is

$$K = F(\theta_o, \theta_n, \beta') = \frac{cF_c - \dfrac{\gamma H\sin(\alpha-\beta')(F_1-F_2-F_3-F_7)}{\sin\beta'\{\sin(\theta_o+\alpha)-\exp[(\theta_h-\theta_o)\tan\phi]\sin(\theta_h+\alpha)\}} - pF_p}{\dfrac{\gamma H\ \sin(\alpha-\beta')(F_4-F_5-F_6-F_8)}{\sin\beta'\{\sin(\theta_o+\alpha)-\exp[(\theta_h-\theta_o)\tan\phi]\sin(\theta_h+\alpha)\}} + \mathrm{x}pF_q} \tag{32}$$

K has a minimum value and, thus, indicates a least upper bound solution when θ_n, θ_o and β' satisfy the following conditions

$$\frac{\partial K_c}{\partial \theta_h} = 0, \quad \frac{\partial K_c}{\partial \theta_o} = 0 \text{ and} \frac{\partial K_c}{\partial \beta'} = 0 \tag{33}$$

From which the minimum value of K, i.e.; K_c is obtained

$$K_c = \text{min. } F(\theta_o, \theta_h, \beta') \tag{34}$$

VI. Numerical Results

Extensive numerical results have been obtained by this program. Some of the results are tabulated in Tables 1 to 6 and illustrated graphically in Fig. 4 to 10.

(A) Homogeneous and Isotropic slopes

(1) Tables 1 (1) and (2) present the yield acceleration factor K_c corresponding to the plane failure mechanism and the log-spiral failure mechanism, respectively. The stability number $N_s = H_c \frac{\gamma}{c}$ is taken to be 6.667 and the surcharge load p is zero.

(2) Tables 2 (a) and (b) present the K_c values corresponding to several sets of N_s and α values. It can be seen by comparing Tables 2 (a) with 2 (b) that K_c of log-spiral failure mechanism is less than that of plane failure mechanism. This shows that log-spiral failure mechanism generally controls the local slope failure. The relationship between the yield acceleration K_c and the stability factor N_s corresponding to the log-spiral failure mechanism is shown in Fig. 4.

(3) Figure 5 (a) and (b) represent the relationship between the K_c values of log-spiral mechanism normalized by the K_c values of plane mechanism and α. These ratios of $K_{c,log} / K_{c,plane}$ are all less than unit, so it shows clearly that the log-spiral failure mechanism generally controls the failure. Figures 6 (a) and (b) and 7 (a) and (b) show the relationships between L/r_o and α and the relationthip between θ_o, θ_h and α, respectively.

(4) Figure 8 presents the stability number N_s for the case where the log-spiral failure plane passing below the toe for three values of ϕ =5°, 10°, 40°, while in Figs. 9 (a) and (b), the relationships between the stability number N_s and the slope angle β are shown.

(5) Tables 3 (a) and (b) compare the solutions for the case where the slip surface passing through the toe with that passing below the toe.
The case controls the failure is denoted by the symbol * in the two tables. Tables4 hows the variation of D/H with respect to changing α and N_s.

(6) Based on these results, the variation of the stability number N_s with yield acceleration K_c is shown in Fig. 10 where the solutions corresponding to the failure mechanism passing through the toe are cut off by the solutions passing below the toe.

(7) The effect of surcharge p and xK on K_c is show in Table 5 again, it is seen that the log-spiral failure mechanism controls the failure where * denotes the case passing below the toe.

(8) A comparison of the present limit analysis solutions with existing limit equilibrium solutions is given in Table 6. The factor of safety obtained for the limit equilibrium solution corresponds to the collapse state of the limit analysis solution. Then, if these solutions are identical, the factor of safety so obtained should be very close to unity.
This procedure is illustrated further by the following example. For the case of xK = o, α = o, ϕ = 40°, c = 900psf, γ = 60pcf, H = 100' and p = 120psf, the value of K_c from limit analysis is used as input data to determine the corresponding factor of safety in STABL program which is a limit equilibrium program developed at Purdue University. Further, note that the circular surface is assumed in the limit equilibrium method, while the log-spiral surface is used in the present limit analysis method. The results are seen somewhat different.

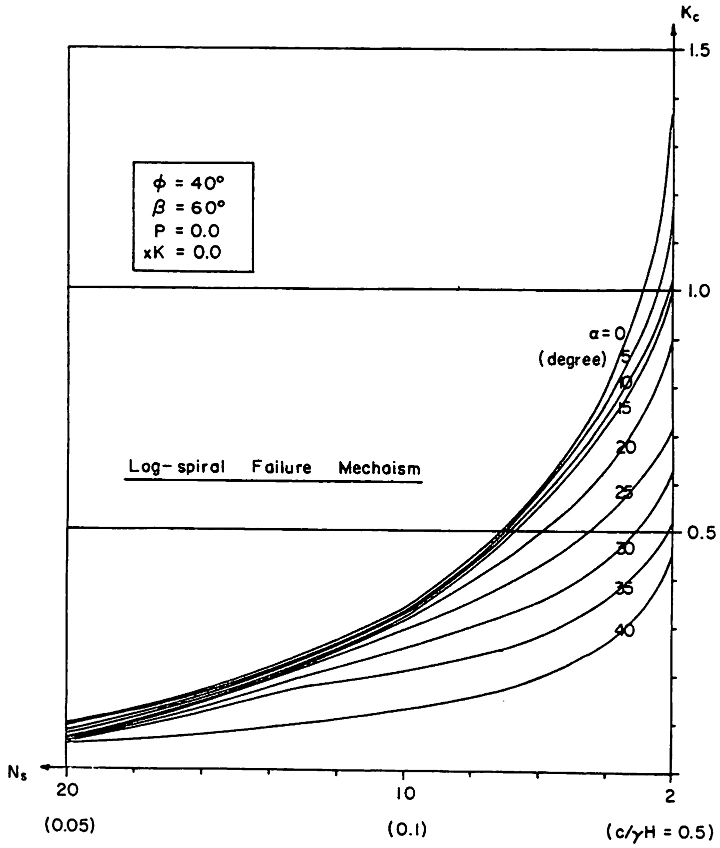

Fig. 4 Relationship Between K_c and N_s

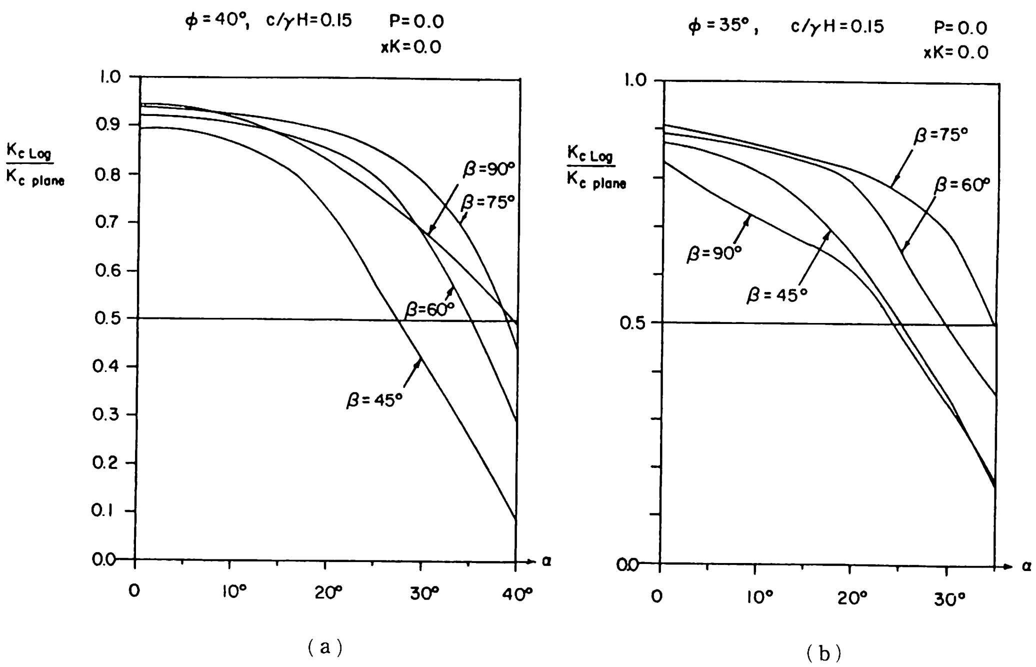

Fig. 5 Relationship Between K_{cLog}/K_{cplane} and α

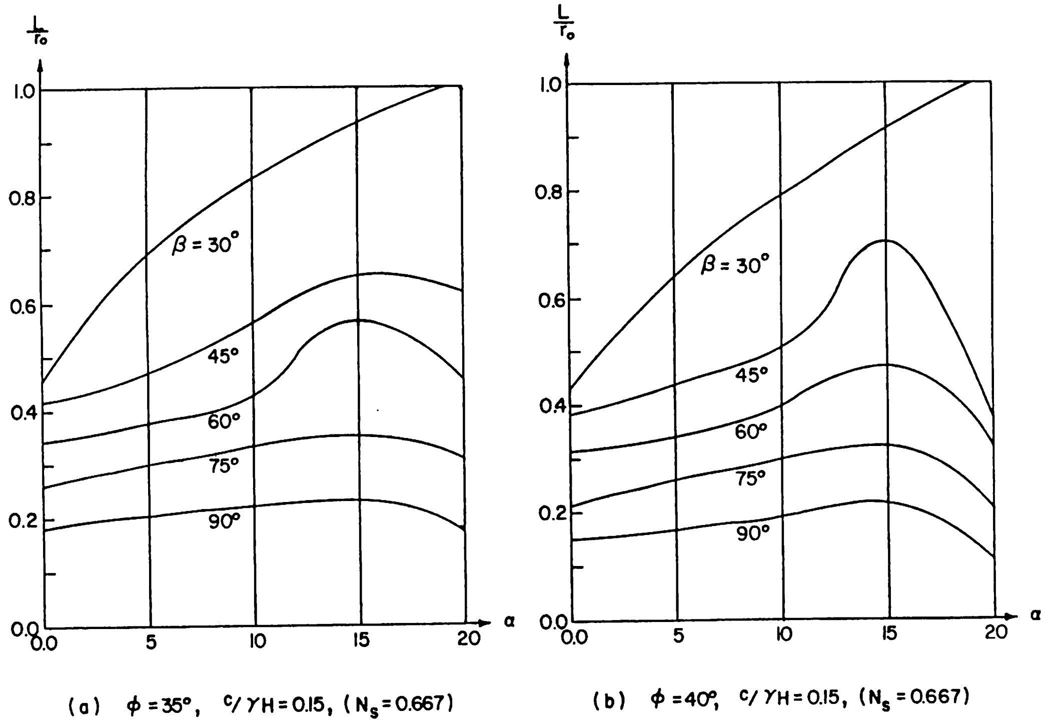

Fig. 6 Relationship Between $\frac{L}{r_0}$ and α.

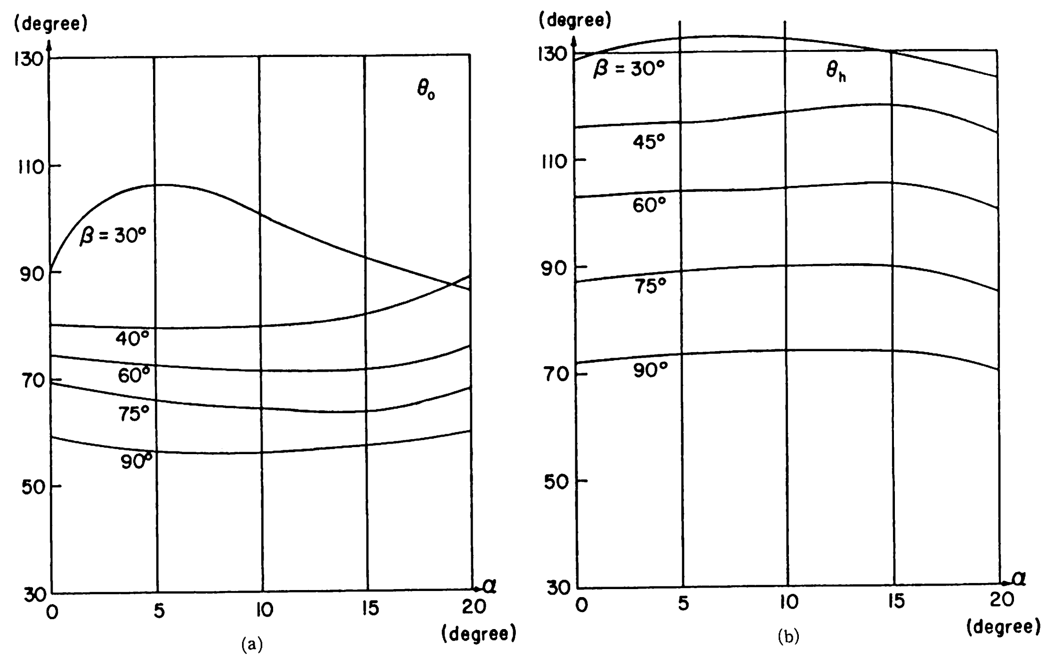

Fig. 7 Relationship Between. θ_0, θ_h and α with $\phi=40^\circ$, c/rH 0.15, ($N_s=0.667$)

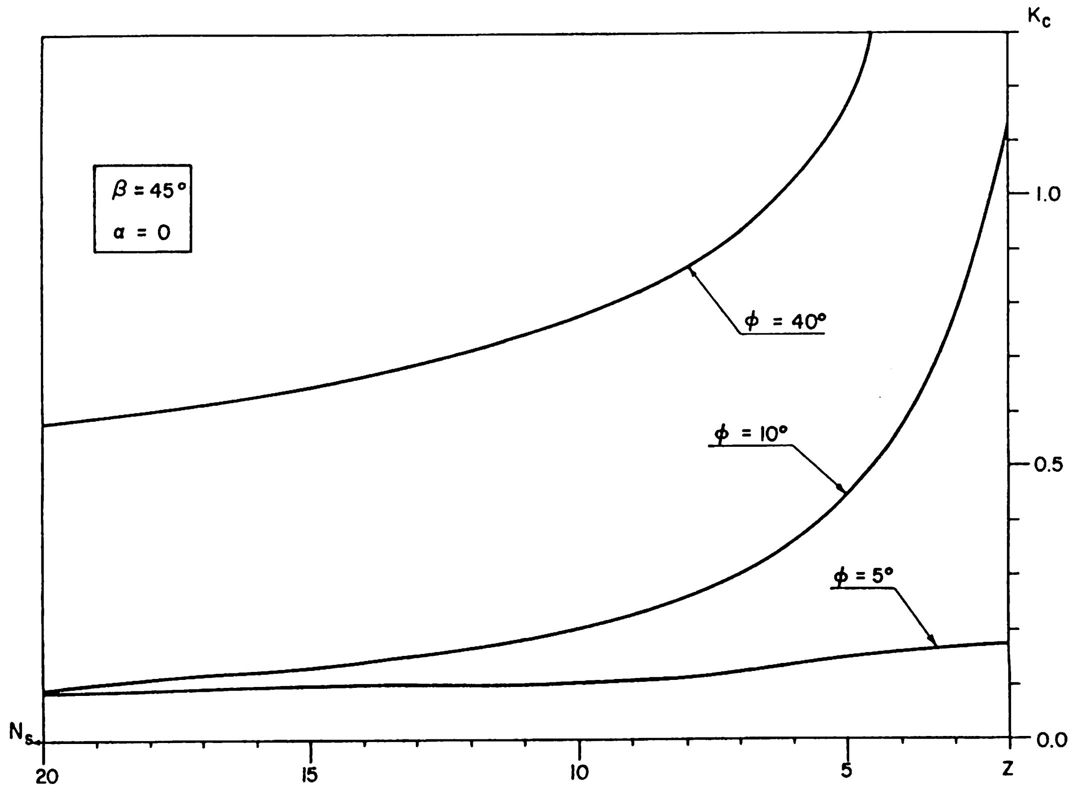

Fig. 8 Comparison with ϕ of K_c

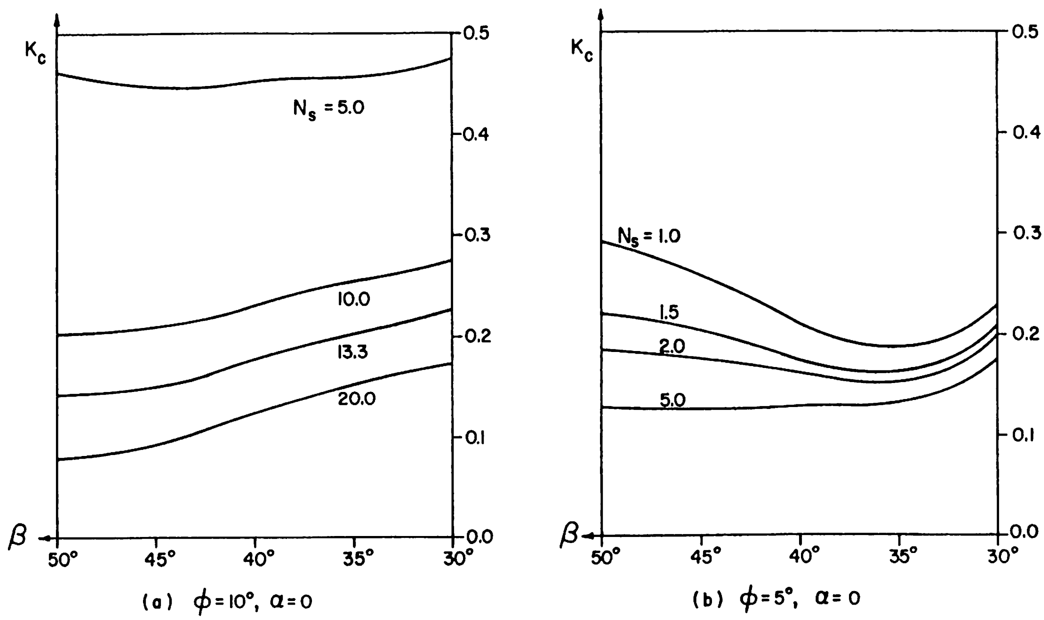

Fig. 9 Relationship Between N_s and β of $- K_c -$

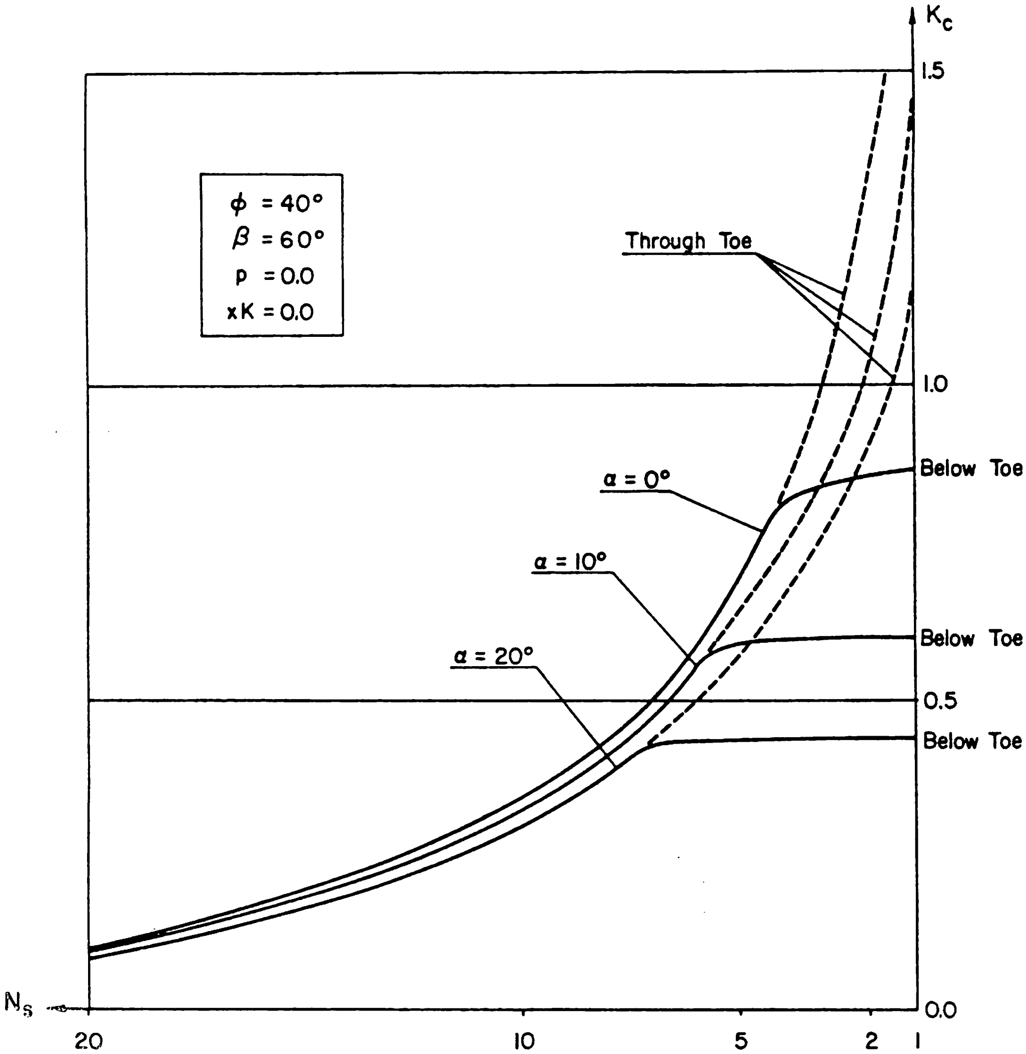

Fig. 10 Relationship Between K_c and N_s

Table 1(a) $-K_c-$for Long$-$Spiral failure mechanism
with $p=0.0$, $xK=0.0$, $N_s=6.667$, $\left(\frac{c}{rH}=0.15\right)$

Friction angle ϕ (degrees)	Slope angle α (degrees)	Slope angle β (degrees)					
		90	75	60	45	30	15
0	0						0.080
5	0				0.098	0.150	0.165
	5				0.051	0.084	0.091
10	0			0.053	0.151	0.221	0.253
	5			0.042	0.143	0.192	0.188
	10			0.027	0.115	0.117	0.124
15	0			0.146	0.253	0.322	0.356
	5			0.135	0.239	0.289	0.291
	10			0.132	0.217	0.215	0.224
	15			0.121	0.132	0.140	
20	0		0.074	0.230	0.343	0.420	0.460
	5		0.066	0.219	0.328	0.391	0.399
	10		0.057	0.206	0.308	0.312	0.324
	15		0.045	0.189	0.227	0.238	
	20		0.034	0.166	0.148	0.164	
25	0		0.148	0.307	0.428	0.517	0.568
	5		0.141	0.300	0.415	0.493	0.496
	10		0.133	0.285	0.395	0.411	0.426
	15		0.123	0.269	0.321	0.333	
	20		0.111	0.246	0.241	0.242	
	25		0.093	0.150	0.163	0.183	
30	0	0.002	0.215	0.380	0.504	0.615	0.683
	5		0.209	0.371	0.499	0.600	0.607
	10		0.202	0.360	0.481	0.513	0.533
	15		0.192	0.345	0.416	0.431	
	20		0.181	0.324	0.335	0.352	
	25		0.165	0.239	0.254	0.277	
	30		0.145	0.160	0.177		
35	0	0.063	0.277	0.449	0.595	0.715	0.811
	5	0.059	0.271	0.441	0.583	0.715	0.725
	10	0.054	0.264	0.431	0.566	0.621	0.645
	15	0.050	0.256	0.420	0.518	0.533	
	20	0.049	0.249	0.402	0.438	0.450	
	25	0.036	0.232	0.329	0.346	0.371	
	30	0.026	0.214	0.248	0.267		
	35	0.014	0.151	0.169	0.190		
40	0	0.116	0.333	0.516	0.677	0.839	0.950
	5	0.113	0.328	0.508	0.666	0.819	0.855
	10	0.110	0.322	0.499	0.651	0.736	0.767
	15	0.109	0.318	0.487	0.627	0.641	
	20	0.106	0.315	0.482	0.552	0.562	
	25	0.094	0.298	0.440	0.444	0.469	
	30	0.086	0.278	0.336	0.358		
	35	0.075	0.235	0.255	0.279		
	40	0.061	0.156	0.177	0.202		

Table 1(b)　$-K_c-$for Plane Failure Mechanism

with p=0.0　xK=0.0

$N_s=6.667,\ \left(\frac{c}{\gamma H}=0.15\right)$

Friction angle φ (degrees)	Slope angle α (degrees)	Slope angle β (degrees)					
		90	75	60	45	30	15
0	0						0.342
5	0			0.105	0.247	0.347	0.426
	5			0.105	0.247	0.347	0.568
10	0			0.181	0.324	0.430	0.511
	5			0.181	0.324	0.430	0.648
	10			0.181	0.324	0.430	1.192
15	0		0.067	0.252	0.399	0.512	0.598
	5		0.067	0.252	0.399	0.512	0.728
	10		0.067	0.252	0.399	0.534	1.258
	15		0.067	0.252	0.399	0.626	
20	0		0.134	0.319	0.472	0.595	0.687
	5		0.134	0.319	0.472	0.595	0.811
	10		0.134	0.319	0.472	0.611	1.324
	15		0.134	0.319	0.472	0.695	
	20		0.134	0.319	0.481	0.935	
25	0		0.195	0.383	0.544	0.679	0.781
	5		0.195	0.383	0.544	0.679	0.896
	10		0.195	0.383	0.544	0.690	1.393
	15		0.195	0.383	0.544	0.765	
	20		0.195	0.383	0.549	0.997	
	25		0.195	0.383	0.595	1.856	
30	0	0.022	0.252	0.444	0.615	0.766	0.822
	5		0.252	0.444	0.615	0.766	0.987
	10		0.252	0.444	0.615	0.772	1.465
	15		0.252	0.444	0.615	0.836	
	20		0.252	0.444	0.617	1.052	
	25		0.252	0.444	0.654	1.865	
	30		0.252	0.444	0.775		
35	0	0.076	0.304	0.502	0.687	0.856	0.991
	5	0.076	0.304	0.503	0.687	0.856	1.084
	10	0.076	0.304	0.503	0.687	0.858	1.540
	15	0.076	0.304	0.503	0.687	0.910	
	20	0.076	0.304	0.503	0.687	1.108	
	25	0.076	0.304	0.503	0.714	1.874	
	30	0.076	0.304	0.503	0.820		
	35	0.076	0.304	0.513	1.119		
40	0	0.124	0.353	0.560	0.759	0.951	1.112
	5	0.124	0.353	0.560	0.759	0.951	1.190
	10	0.124	0.353	0.560	0.759	0.951	1.622
	15	0.124	0.353	0.560	0.759	0.989	
	20	0.124	0.353	0.560	0.759	1.166	
	25	0.124	0.353	0.560	0.775	1.883	
	30	0.124	0.353	0.560	0.865		
	35	0.124	0.353	0.564	1.135		
	40	0.124	0.353	0.610	2.117		

Table 2(a) Comparison with Ns for Lg-spiral Failure Mechanism

with $\phi=40°$, $\beta=60°$

p=0.0, xK=0.0

	Log-spiral Failure Mechanism $-K_c-$					
N_s / α	2.0 (c/γH=0.5)	5.0 (3/γH=0.2)	6.667 (c/γH=0.15)	10.0 (c/γH=0.1)	13.333 (c/γH=0.075)	20.0 (c/γH=0.05)
0°	1.354	0.668	0.516	0.335	0.225	0.096
5°	1.171	0.657	0.508	0.331	0.223	0.094
10°	1.035	0.643	0.499	0.325	0.220	0.093
15°	0.915	0.623	0.487	0.319	0.216	0.091
20°	0.807	0.557	0.482	0.311	0.210	0.088
25°	0.710	0.467	0.444	0.299	0.203	0.085
30°	0.620	0.382	0.336	0.281	0.193	0.080
35°	0.536	0.301	0.255	0.205	0.177	0.072
40°	0.457	0.223	0.177	0.127	0.099	0.060

Table 2(b) Comparison with Ns for plane Failure Mechanism

with $\phi=40°$, $\beta=60°$

p=0.0, xK=0.0

	Plane Failure Mechanism $-K_c-$					
N_s / α	2.0 (c/γH=0.5)	5.0 (3/γH=0.2)	6.667 (c/γH=0.15)	10.0 (c/γH=0.1)	13.333 (c/γH=0.075)	20.0 (c/γH=0.05)
0°	1.458	0.711	0.560	0.388	0.287	0.170
5°	1.458	0.711	0.560	0.388	0.287	0.170
10°	1.458	0.711	0.560	0.388	0.287	0.170
15°	1.458	0.711	0.560	0.388	0.287	0.170
20°	1.461	0.711	0.560	0.388	0.287	0.170
25°	1.499	0.711	0.560	0.388	0.287	0.170
30°	1.595	0.712	0.560	0.388	0.287	0.170
35°	1.781	0.738	0.564	0.388	0.287	0.170
40°	2.117	0.826	0.610	0.395	0.287	0.170

Table 3(a) Comparison between through toe and below toe of $-K_c-$with $\phi=10°$ $\beta=60°$

α \ N_s		1.0 c/γH (1.0)	1.5 (0.667)	2.0 (0.5)	2.5 (0.5)	5.0 (0.2)	6.667 (0.15)
0°	*(1)	0.925	0.676	0.552	0.478	0.323	0.053
	(2)	2.863	1.520	1.142	0.917	0.515	0.368
5°	*(1)	0.818	0.581	0.462	0.390	0.214	0.042
	(2)	2.452	1.561	1.160	0.779	0.397	0.275
10°	(1)	0.727	0.496	0.375	0.306	0.186	0.027
	*(2)	0.492	0.346	0.273	0.226	0.141	0.081

(1) : Through Toe

(2) : Below Toe

* : Control the failure

Table 3(b) Comparison between Through Toe and Below Toe of $-K_c-$ with $\phi=40°$, $\beta=60°$

α \ N_s		1.0 c/δH (1.0)	2.0 (0.5)	5.0 (0.2)	6.67 (0.15)	10.0 (0.1)	13.33 (0.075)	20.0 (0.05)
0°	(1)	1.788	1.354	*0.668	*0.516	*0.335	*0.225	*0.096
	(2)	*0.861	*0.852	0.849	1.401	1.060	0.887	0.716
5°	(1)	1.597	1.171	*0.657	*0.508	*0.331	*0.223	*0.094
	(2)	*0.720	*0.714	0.709	0.706	0.706	0.706	0.656
10°	(1)	1.434	1.035	0.643	*0.499	*0.325	*0.220	*0.093
	(2)	*0.598	*0.595	*0.594	0.593	0.593	0.593	0.609
15°	(1)	1.293	0.915	0.623	*0.487	*0.319	*0.216	*0.091
	(2)	*0.502	*0.501	*0.501	0.500	0.500	0.500	0.500
20°	(1)	1.170	0.807	0.557	0.482	*0.311	*0.210	*0.088
	(2)	*0.425	*0.424	*0.424	*0.424	0.423	0.423	0.423

(1) : Through Toe

(2) : Below Toe

* : Control the failure

Table 4 Variation of D/H with α and N_s

α (degrees) \ N_s	1.0 $\frac{1}{N_s}$ (1.0)	2.0 (0.5)	2.5 (0.4)	4.0 (0.25)	5.0 (0.2)	6.667 (0.15)
0	0.547	0.467	0.458	--	--	--
5	0.351	0.311	0.262	--	--	--
10	0.262	0.262	0.262	0.262	0.262	--
15	0.262	0.262	0.262	0.262	0.262	--
20	0.262	0.262	0.262	0.262	0.262	0.262

Table 5 $-K_c-$ Comparison between p and xK with $N_s = 6.667$, $\left(\frac{c}{\gamma H} = 0.15\right)$ $\phi = 40°$, $\beta = 60°$

	p = 0.0 xK = 0.0		p = 120 psf xK = 0.0		p = 120 psf xK = 0.5	
Slope angle α (degrees)	plane	log-spiral	plane	log-spiral	plane	log-spiral
0	0.560	0.516*	0.563	0.513*	0.552	0.506*
5	0.560	0.508	0.563	0.505	0.552	0.499
10	0.560	0.499	0.564	0.496	0.551	0.490
15	0.560	0.487	0.564	0.484	0.550	0.477
20	0.560	0.482	0.564	0.467	0.549	0.461
25	0.560	0.444	0.565	0.443	0.548	0.436
30	0.560	0.336	0.565	0.339	0.546	0.336
35	0.564	0.225	0.568	0.257	0.546	0.255
40	0.610	0.177	0.607	0.177	0.577	0.176

*Below Toe

Table 6 Factor of Safety Obtained by Limit Equilibrium Method

β (degrees)	15	30	45	60	75	90
Factor of Safety	0.920	0.885	0.891	0.933	1.006	1.025

Appendices

Physical Limits and Constraints

Several physical constraints as imposed by the geometrical consideration of the failure mechanisms must be included in the programs in order to effectively execute OPTIMIZATION techniques. These conditions are considered separately for the following three cases.

Case 1: plane failure mechanism and log-spiral failure mechanism passing through the toe for homogeneous and anisotropic slopes

One constraint for the translational failure mechanism and four constraints for the rotational failure mechanism are identified from the physical considerations. Referring to Fig. 1 and 2, these conrstaints are:

(1) The rate of external work done by the inertia force KW must be positive, that is, the inertia force must be moving away from the slope in order to reduce the stability of the slope;

(2) The yield acceleration factor, K_c, must be positive;

(3) In case of the rotational failure mechanism, the conditions H/r_0 and L/r_0 must be positive;

Case 2: log-spiral failure mechanism passing below the toe for a homogeneous and isotropic slopes

(4) In addition to items (1), (2) and (3), the conditions D/H must be positive, if this failure mechanism is a possibility (Fig. 3).

(5) Tce geometrical relationship of L and H, D and H must be specified according to an actual soil profile or boundary conditions, so that a desirable praactical solution can be resulted. For some combiations of $\frac{\gamma H}{c}$ or N_s, ϕ, β and α, the minimum K_c value can be associated with an infinite value of L/H and D/H ratios. This is the reason why an upper limit of L/H and D/H must be specified in order to confine the numerical results within a reasonable range.

REFERENCES

1) Chen, W.F. :"Limit Analysis and Soil Plasticity", Elsevier Scientific Publishing Co., Amsterdam, Netherland, 1975.

2) Chen, W.F. :"Limit Analysis of Stability of Slopes", Journal of the Soil Mechanics and Foundation Division, ASCE, Vol.97, No.SMI,1971.

3) Sigel, R.A. :"STABL user Manual", Joint Highway Research Project, JHRP-75-9, School of Civil Engineering, Purdue University, 1978.

4) Chen, W. F. and Sawada, T. : "On Analysis of Seismic Stability of Slopes in Anisotropic Soils", Technical Report-CE-STR- 82-25, Purdue University Structural Engineering, 1982.

5) Sawada, T., Nomachi, S. G. and Chen, W. F. : "Seismic Stability of Nonhomogeneous, Anisotropic Slopes", E. M. D. Speciality Conference, ASCE, 1983.

6) Gabriele, G. A. and Pagsdell, K. M. : "OPT : A Nonlinear Programming Code in Fortran-IV User's Manual", The Modern Design Series, Purdue Research Foundation C, school of Mechanical Engineering, Purdue University, 1976.